Backscattering coefficients for low energy positrons and electrons impinging on bulk solid targets

2009 J. Phys.: Condens. Matter 21 095403

(http://iopscience.iop.org/0953-8984/21/9/095403)

J. Phys.: Condens. Matter **21** (2009) 095403 (5pp) doi:10.1088/0953-8984/21/9/095403

Backscattering coefficients for low energy positrons and electrons impinging on bulk solid targets

A Bentabet[1] **and N Fenineche**[2]

[1] Département SM, Centre Universitaire de BBA, Algeria
[2] Université de Technologie, Belfort-Montbéliard, France

Received 30 August 2008, in final form 15 January 2009
Published 30 January 2009
Online at stacks.iop.org/JPhysCM/21/095403

Abstract
The backscattering coefficients (BSCs) for semi-infinite solids of normally incident 1–4 keV electrons and positrons are stochastically modeled and calculated by the Monte Carlo method. This paper aims at discussing the differences observed between the properties of electrons and positrons impinging on solid targets based on the use of the differential elastic scattering cross-section which has been obtained using the Bentabet and Bouarissa approximation (2006 *Phys. Lett.* A **355** 390). A new mathematical equation was developed for the adjustable parameter β of the Bentabet *et al* approximation and seems to be valid for other elements. Both electron and positron BSC simulated results show good agreement with the experimental or computed data reported by other authors.

1. Introduction

Electron– and positron–material interaction has a great importance in many domains of analytical techniques such as electron probe microanalysis, Auger electron spectroscopy, positron annihilation spectroscopy, scanning electron microscopy (SEM) etc [1–10]. The Monte Carlo method has become a powerful tool for carrying out such study. The Monte Carlo programs used in the models of the electron and positron implantation profile were developed first by Valkealahti and Nieminen [11, 12], Adesida *et al* [13], Jensen and Walker [4, 6], Fernandez-Varea *et al* [14] and Lynn and McKeown [15]. All these programs have a similar structure. The accuracy of the model which is used depends on the modeling of scattering processes included in the study of the projectile particle–material interaction. The most dominant interactions are the elastic and inelastic processes. Among the most successful methods in determining the electron and the positron elastic cross-sections is the RPWEM (relativistic partial wave expansion method) [16, 17]. However, the projection in the Monte Carlo code requires a very long time compared to analytical expressions.

The model that we have used in this study is similar to that explained in our articles published recently [19–23] using the Bentabet *et al* approximation to calculate the elastic differential cross-section [21]. This approximation is an analytical expression with an adjustable parameters compared to RPWEM.

In the present work, we have calculated the BSC for semi-infinite solid targets of the following samples: Al (light element), Au (heavy element) and Cu (intermediate element) in the energy range (0.1–4 keV). This latter BSC is a major factor to validate the model used in the simulation and highlights the absorbed rate of incident particles [18]. Backscattered electrons (positrons) are the particles of an electron (positron) beam that return and emerge from a target surface when the beam impinges on a solid.

In the present work, we have almost explained the majority of differences observed between the electron BSC and the positron BSC, in the solid, referring to the $\exp(\alpha - \beta\theta)$ term of the Bentabet *et al* approximation. In addition, an analytical expression relating to the β parameter has been developed and could be generalized for other solids. Moreover, results obtained are in agreement with those of the literature.

2. Method

The elastic differential cross-sections which are used to describe the interaction of both electrons and positrons with solid targets are calculated with the same method of approximation as explained in [21]. This approximation suggests that the elastic differential cross-section can be

written in the following form:

$$\frac{\mathrm{d}\sigma_{\mathrm{el}}(\theta)}{\mathrm{d}\Omega} = \mathrm{e}^{\alpha-\beta\theta}\left.\frac{\mathrm{d}\sigma_{\mathrm{el}}(\theta)}{\mathrm{d}\Omega}\right|_{\mathrm{R}}, \tag{1}$$

where α and β are two adjustable parameters which depend on the characteristics of the studied material and the kinetic energy of both incident electron and positron, and $\frac{\mathrm{d}\sigma_{\mathrm{el}}(\theta)}{\mathrm{d}\Omega}|_{\mathrm{R}}$ is the screened Rutherford cross-section.

The α parameter is given by

$$\alpha = \ln\left\{\frac{\sigma(E)}{\int_0^{\pi} 2\pi, \sin\theta\, \mathrm{e}^{-\beta\theta}\left.\frac{\mathrm{d}\sigma_{\mathrm{el}}(\theta)}{\mathrm{d}\Omega}\right|_{\mathrm{R}}}\right\}, \tag{2}$$

where $\sigma(E)$ is the total cross-section obtained by the relativistic partial wave expansion method (RPWEM) which was reported by Dapor [26].

The use of the Bentabet *et al* approximation is tested, to study the electron (positron) transport in a solid target, for *energies lower than or equal to* 4 keV either by using an analytical method [22, 23] like that developed by Vicaneck and Urbassek [24] or the stochastic Monte Carlo method [21–23, 25]. In addition, the analytical expression (equation (1)) could be valid for higher energies. However, the determination method of the beta parameter, particularly in the electron case, must be changed due to the influence of the particle energy and the relativistic effects on the elastic cross-section.

The core and the valence electron excitations are described using Gryzinski's excitation function [27–29]. The Gryzinski's differential cross-section is given by the following expression:

$$\frac{\mathrm{d}\sigma(\Delta E)}{\mathrm{d}(\Delta E)} = \pi\frac{e^4}{\Delta E^3}\frac{E_{\mathrm{B}}}{E}\left(\frac{E}{E+E_{\mathrm{B}}}\right)^{3/2}\left(1-\frac{\Delta E}{E}\right)^{\frac{EB}{EB+\Delta E}} \times \frac{\Delta E}{E_{\mathrm{B}}}\left(1-\frac{E_{\mathrm{B}}}{E}\right)+\frac{4}{3}\ln\left(2.7+\left[\frac{E-\Delta E}{E_{\mathrm{B}}}\right]^{1/2}\right), \tag{3}$$

where ΔE, E_{B} and E are the energy loss, the mean electron binding energy and the primary projectile energy respectively.

The total inelastic cross-section is given as

$$\sigma_{\mathrm{inél}} = \pi\cdot e^4 N_{\mathrm{S}}\left(\frac{E-E_{\mathrm{B}}}{E+E_{\mathrm{B}}}\right)^{3/2}\left\{1+\frac{2}{3}\left(1-\frac{E_{\mathrm{B}}}{2E}\right)\cdot\ln\left[2.7+\left(\frac{E}{E_{\mathrm{B}}}-1\right)^{1/2}\right]\right\}, \tag{4}$$

where N_{S} is the number of electrons in a particular 'shell' contributing to the inelastic events.

The energy loss is taken equal to zero if it is less than the mean binding energy of an electron of the target atom.

It should be noted that Gryzinski's model focuses on the difference between core and valence electron interactions. Consequently, one can get more information on the contribution of each type of collision. However, several other models neglected the core electron contribution or introduce it in a total expression reflecting the inelastic effect—mean free path, stopping power, inelastic cross-section, etc, like Bethe theory [30], Kanaya and Okayama's semi-empirical formula [31], Penn's model [32], Ashley's optical model [33], etc.

Although it is in some cases sufficient to treat the inelastic scattering of charged particles in a continuous slowing down approximation [34], the most accurate Monte Carlo method describes both elastic and inelastic scattering as discrete events [35].

These electrons (positrons) are not reflected without dissipation of energy because of their penetration below the surface and the resulting loss of small amounts of energy through ionization, electron excitations and plasmon emissions. A fraction of the energy is in fact lost in the solid before emerging [51]. The plasma oscillations could be considered as quantified particles named plasmons. The plasmon energy is about 15.3 eV in aluminum and 14.07 eV in Au. Generally, this *latter* effect could be neglected in equilibrium metal.

3. Computation

The Monte Carlo method has also been used to study the charged particle transportation in bulk solid targets by identifying the trajectories followed by the incident particle. The electrons as well as the positrons since their penetration through the external surface to the end of their history will be defined by one of the following three cases.

If the incident particle loses its energy through the inelastic process inside the solid target to the point that its energy is inferior or equal to 100 eV then it is an absorbed particle. If it retreats from the same surface through which it penetrated then it is a backscattered particle and if it crosses the film thickness then it is a transmitted particle. The Monte Carlo method uses uniform random numbers belonging to the interval [0–1]. In the simulation, five random numbers were used to study the trajectories of the electrons or positrons in the solid target. Briefly, the Monte Carlo program uses five random numbers, namely $R_1, R_2, \ldots, R_5$ for identifying random events that contribute to the transport model: the type of collision, either elastic or inelastic (either with core electrons or valence electrons), the distance between the two successive collisions, the diffusion angle after an elastic collision, the energy loss in the case of an inelastic collision, and the *azimuthal* angle after every collision either elastic or inelastic. The random numbers $R_1, R_2, \ldots, R_5$ are introduced as follows.

- The distance between the two successive collisions named (S) is calculated as follows:

$$S = -\lambda_T \ln(R_1), \tag{5}$$

where λ_T is the total mean free path given as

$$\frac{1}{\lambda_T} = \frac{1}{\lambda_{\mathrm{el}}} + \frac{1}{\lambda_{\mathrm{c}}} + \frac{1}{\lambda_{\mathrm{v}}}, \tag{6}$$

where λ_{el}, λ_{c} and λ_{v} are the mean free paths, elastic and inelastic of core electrons and inelastic of valence electrons respectively.

Table 1. The parameter β of the Bentabet and Bouarissa approximation. (Note: E (keV) is the primary energy.)

		β(rad^{-1}) case	
	Particle	β constant	β versus energy (keV)
Al	Electron	0.36	$-0.085 + 0.47E - 0.09E^2$
	Positron	1.782	$1.332 + 0.736\exp(-(10^3E - 671.386)/2100.382)$
Cu	Electron	0.64	$-0.43 + 1.1E - 0.20E^2$
	Positron	2.697	$1.992 + 0.852\exp(-(10^3E - 1285.836)/1257.825)$
Au	Electron	1.09	$-1.46 + 2.59E - 0.45E^2$
	Positron	3.523	$0.708 + 4.3E - 1.726E^2 + 0.2138E^3$

- The type of collision is defined as follows.

  If
$$R_2 \leqslant \frac{1/\lambda_{el}}{1/\lambda_T} \tag{7}$$
  the collision is elastic.

  If
$$\frac{1/\lambda_{el}}{1/\lambda_T} < R_2 \leqslant \frac{1/\lambda_{el} + 1/\lambda_c}{1/\lambda_T} \tag{8}$$
  the collision is inelastic with the core electrons.

  If
$$R_2 > \frac{1/\lambda_{el} + 1/\lambda_c}{1/\lambda_T} \tag{9}$$
  the collision is inelastic with the valence electrons.
- The diffusion angle after every elastic collision is given as
$$R_3 = \frac{\int_0^\theta \frac{d\sigma}{d\Omega}\, d\Omega}{\sigma_{el}}. \tag{10}$$
- The energy loss after every inelastic collision is given as
$$R_4 = \frac{\int_{\Delta E}^{E} \frac{d\sigma_{inel}}{d(\Delta E)}\, d(\Delta E)}{\sigma_{inel}}. \tag{11}$$
- The *azimuthal* angle is given as
$$R_5 = \frac{\varphi}{2\pi}. \tag{12}$$

Diffusion angle after an inelastic collision is expressed by the expression of binary collision model given as follows:

$$\theta = \arcsin\left(\sqrt{\frac{\Delta E}{E}}\right). \tag{13}$$

In our simulation the *termination* energy was chosen to be 100 eV. The choice of the termination energy does not have much effect, since the path length traveled by the electron between 100 eV and near thermal energies is insignificant (a few angstroms) compared to the implantation depths [35–37].

Phonon scattering does not contribute to the projected ranges but will gradually lead to the random walk blurring of the implantation profile. As the particles will eventually start to diffuse around the endpoints of their trajectories, as phonon scattering becomes weaker at low temperatures, the blurring effect (and the diffusion constant) becomes larger [11].

In the case of the Monte Carlo method the statistical error is calculated as $1/\sqrt{N}$, where N is the number of initial particles. Since 10^5–10^6 particle histories were used, this statistical error is found to be about 0.1%.

Table 2. Backscattering coefficients (BSCs) of 1–4 keV electrons impinging on semi-infinite Al, Cu and Au: present calculation (PW [21]) compared to theoretical [20, 26] and the experimental data estimated from the curves reported in [38]. (Note: PW1, present work in the β constant case; PW2, present work in the β versus energy case.)

		E (keV)			
		1	2	3	4
Aluminum	PW1	0.185	0.176	0.172	0.172
	PW2	0.192	0.165	0.152	0.167
	Exp. [38]		0.175	0.170	0.165
	Reference [20]	0.195	0.180	0.176	0.164
	Reference [26]	0.197	0.187	0.181	0.178
Copper	PW1	0.292	0.293	0.296	0.296
	PW2	0.313	0.269	0.238	0.272
	Exp. [38]		0.3	0.30	0.3
	Reference [20]	0.329	0.325	0.307	0.29
	Reference [26]	0.315	0.314	0.312	0.312
Gold	PW1	0.331	0.382	0.413	0.432
	PW2	0.36	0.332	0.272	0.378
	Exp. [38]		0.375	0.410	0.430
	Reference [26]	0.331	0.390	0.414	0.427

4. Results and discussion

The following results have been obtained for a normal incidence and energies lower than or equal to 4 keV electrons and positrons.

In the case of a semi-infinite solid, crossed by a slow particle of low energy; the BSC is the probability for a retreating incident particle from the crossed solid. This means that the diffusion angle of the particle is more than 90°. In the present work, we have used Bentabet's *et al* approximation [21], using the β parameter like a constant and then dependent on energy. The choice between the two situations will be closely connected to the experimental database. We have used BSC experimental data like a criterion of validation. Table 1 presents the parameter β for both cases: β constant and β versus the energy E expressed in keV.

Tables 2 and 3 represent the BSC of electrons and positrons impinging on the aluminum, copper and gold respectively. The results for the electron case have been already discussed in a previous paper [21].

In the positron case one can note when β dependent on energy experimental data are close to those of β constant. Indeed, this energy dependence is very useful to explain the BSC increases in the Al case despite the weakness of the

Table 3. Backscattering coefficients (BSCs) of 1–4 keV positrons impinging on semi-infinite Al, Cu and Au: present calculation (PW) compared to theoretical [39–41] and the experimental data [39]. (Note: PW1, present work in the β constant case; PW2, present work in the β versus energy case.)

		E (keV)			
		1	2	3	4
Aluminum	PW1	0.088	0.085	0.089	0.092
	PW2	0.080	0.089	0.092	0.097
	Exp. [39]	0.069		0.086	
	Reference [39]	0.109		0.115	
	Reference [40]	0.104		0.115	
	Reference [41]	0.118		0.123	
Copper	PW1	0.147	0.156	0.157	0.169
	PW2	0.130	0.166	0.183	0.202
	Exp. [39]	0.135		0.177	
	Reference [39]	0.156		0.194	
	Reference [40]	0.152		0.188	
	Reference [41]	0.122		0.138	
Gold	PW1	0.129	0.189	0.234	0.266
	PW2	0.1335	0.157	0.212	0.256
	Exp. [39]	0.123		0.186	
	Reference [39]	0.168		0.242	
	Reference [40]	0.165		0.232	
	Reference [41]	0.179		0.239	

cross-section. Meanwhile, we can also explain the behavior difference between Cu and Au BSCs for lower energies. The BSC either for electrons or positrons increases from aluminum to copper then to gold. In other words, it can be noted that the BSC of electrons and positrons accordingly increases with the atomic number. The aforementioned fact is justified by the increase of the atomic number, which leads to the increase of the mass density and the elastic cross-sections except for few elements. The BSC increase according to the atomic number has already been proved theoretically as well as experimentally by several authors: Coleman *et al* [39], Ghosh and Aers [41], Mäkinen *et al* [18], Sempau *et al* [42], Aydin [45], Dapor ([43, 44], particularly for primary energies superior to 2 keV). In addition, the BSC of electrons increases with the energy in heavy materials such as gold, decreases in the case of light materials such as aluminum and varies slowly in the intermediate materials such as copper. This can be justified by the fact that heavy atoms have big cross-sections and consequently there is a great probability of diffusion by large angles, in contrast to the case of light materials.

However, in the positron case, BSC increases in a monotonic way with the incident energy, this is justified as follows.

For gold, it is justified by the same argument as mentioned in the case of electrons, i.e. gold atoms have big cross-sections and consequently a great probability of diffusion by large angles. On the other hand, one can justify the BSC behavior versus energy in aluminum and copper cases: the energy increases lead to a decrease of β (see figure 1) and consequently to an increase in the diffusion probability by large angles. Also, the BSC for copper is greater than for gold for some energies (see table 3) although the gold mass density is greater than copper, shown by the β oscillations in the gold

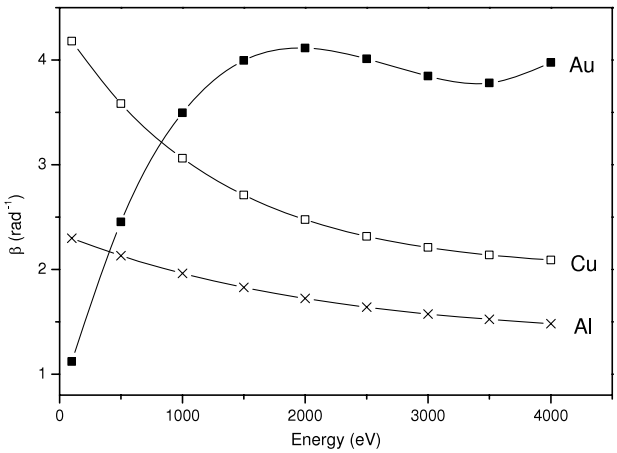

Figure 1. The parameter β versus the incident energy positrons.

case (figure 1). Moreover, the BSC for electrons is greater than for positrons due to the fact that the diffusion probability by small angles is larger compared to electrons and positrons could deepen more inside the solid target.

Thus, the only term which made a difference between electron and positron BSC in the simulation is $\exp(\alpha - \beta\theta)$ which is related to the differential elastic cross-section and consequently to the mean free path, the collision type, the distance covered between two successive collisions etc.

One can note that Bentabet's *et al* approximation is an extension of the formula developed theoretically by Seltzer [46] and given by

$$\frac{\mathrm{d}\sigma}{\mathrm{d}\Omega} = z^2 r_0^2 \frac{\left(1-\gamma^2\right)}{\gamma^4(1-\cos\theta+2\beta_n)} K_{\mathrm{rel}}(\theta, E), \qquad (14)$$

where $z^2 r_0^2 \frac{(1-\gamma^2)}{\gamma^4(1-\cos\theta+2\beta_n)}$ is the screened Rutherford cross-section and $K_{\mathrm{rel}}(\theta, E)$ is the spin-relativistic factor chosen in the Bentab *et al* approximation as $\exp(\alpha-\beta\theta)$; Z is the atomic number of the considered element; r_0 is the classical electron radius ($2\,817\,938 \times 10^{-13}$ cm); γ is the ratio of the initial electron velocity to the velocity of light ($\gamma = v/c$); θ is the scattering angle; β_n is the screening parameter.

Among approximations used to determine $K_{\mathrm{rel}}(\theta, E)$, Aydin's [47–49] is given by

$$K_{\mathrm{rel}}(\theta, E) = \sum_{i=0}^{3} p_i(E)\,\theta^i \qquad (15)$$

θ is the scattering angle and $p_i(E)$ is a free parameter which depends on the energy. This latter ($p_i(E)$) is generally expressed in a polynomial form containing three to four free parameters. Consequently, equation (15) gives from 12 to 16 free parameters in order to evaluate the expression of $K_{\mathrm{rel}}(\theta, E)$. However, the Bentabet *et al* approximation is very useful for this study: on the one hand, it explains the difference of the behavior between positrons and electrons impinging on the solid. On the other hand, it depends only on one parameter to determine (β).

Indeed, the β parameter value is closely equal to 0.36, 0.64 and 1.097 (respectively in Al, Cu and Au). The value

Table 4. Backscattering coefficients (BSCs) of 1–4 keV electrons impinging on semi-infinite Be, Si, Ge and Ag.

E (keV)	Be	Si	Ge	Ag
1	0.071	0.225	0.291	0.315
2	0.058	0.215	0.306	0.352
3	0.052	0.208	0.307	0.360
4	0.052	0.20	0.309	0.365

of β seems to be correlated to the mass density (ρ) and atomic number (Z) by the following equation:

$$\beta\,(Z,\rho) = \exp(-2.0769 + 0.2952\ln(\rho Z)), \qquad (16)$$

where ρ is the mass density (g cm^{-3}) of the studied element.

To test the validity of this equation for other elements (metals and semiconductors), we have calculated the BSC according to primary energy of the electrons in Be, Si, Ge and Ag and results are presented in table 4. Our results agreed with those of the literature (experimental and theoretical; see [26, 42–50] and references therein).

5. Conclusion

In conclusion, we have calculated the BSCs of electrons and positrons backscattered from Al, Cu and Au by using the Monte Carlo simulation method. Therefore, comparing the results with the experimental values we can deduce that the β parameter of the approximation must be constant and independent of energy in the electron case. This parameter was equal to 0.36, 0.64 and 1.09 in the Al, Cu and Au cases and also where the value of β is correlated to the mass density and atomic number by the relation $\beta(Z,\rho) = \exp(-2.0769 + 0.2952\ln(\rho Z))$. In the positron case one can note that when β is dependent on energy it seems to be closer to the experimental data compared to β constant. Indeed, this energy dependence is very useful to explain the BSC increase in the Al case despite the weakness of the cross-section. Meanwhile, we can also explain the behavior difference between the Cu and Au BSC for lower energies. When analyzing the obtained results and the experimental database we can note that obviously the results are in good agreement with the experimental results regarding those found by other authors, which proves the validity of the model. Moreover, the results show the efficiency of the approximation when we study the transport of both electrons and positrons.

References

[1] E.g. see, Lynn KG and McKee B T A 1979 *J. Appl. Phys.* **19** 247
[2] Mills A P Jr 1995 *Positron Spectroscopy of Solids* ed A Dupasquier and A P Mills Jr (Amsterdam: IOS) p 209
[3] Schultz P J and Lynn K G 1988 *Rev. Mod. Phys.* **60** 701
[4] Jensen K O, Walker A B and Bouarissa N 1990 *AIP Conf. Proc.* **218** 19
[5] Massoumi G R, Hozhabri N, Jensen K O, Lennard W N, Lorenzo M S, Schultz PJ and Walker A B 1992 *Phys. Rev. Lett.* **68** 3873
[6] Jensen K O and Walker A B 1993 *Surf. Sci.* **292** 83
[7] Aers G C 1994 *Appl. Phys. Lett.* **64** 661
[8] Dapor M 1995 *J. Appl. Phys.* **77** 2840
[9] Bouarissa N, Walker A B and Aourag H 1998 *J. Appl. Phys.* **83** 3643
[10] Chaoui Z and Bouarissa N 2004 *J. Appl. Phys.* **96** 807
[11] Valkealahatni S and Nieminen R M 1983 *Appl. Phys.* A **32** 95
[12] Valkealahati S and Nieminen R M 1984 *Appl. Phys.* A **35** 51
[13] Adesida I, Shimizu R and Everhart T E 1980 *J. Appl. Phys.* **51** 5962
[14] Fernandez-Varea J M, Liljequist D, Csillag S, Räty R and Salvat F 1996 *Nucl. Instrum. Methods Phys. Res.* B **108** 35
[15] Ritley K A, McKeown M and Lynn K G 1990 *Positron Beams for Solid and Surfaces* ed P J Schultz, G Massoumi and P J Simpson (New York: AIP) p 3
[16] Salvat F, Jablonski A and Powell C J 2005 *Comput. Phys. Commun.* **165** 157
[17] Mayol R and Salvat F 1997 *At. Data Nucl. Data Tables* **65** 55
[18] Mäkinen J, Palko S, Martikainen J and Hautjarvi P 1992 *J. Phys.: Condens. Matter* **4** L503
[19] Deghfel B, Bouarissa N and Bentabet A 2003 *Phys. Status Solidi* b **238** 136
[20] Bouarissa N, Deghfel B and Bentabet A 2002 *Eur. Phys. J.* AP **19** 89
[21] Bentabet A and Bouarissa N 2006 *Phys. Lett.* A **355** 390
[22] Bentabet A and Bouarissa N 2007 *Surf. Interface Anal.* **39** 377
[23] Bentabet A and Bouarissa N 2007 *Appl. Phys.* A **88** 353
[24] Vicanek M and Urbassek H M 1991 *Phys. Rev.* B **44** 7234
[25] Bentabet A and Bouarissa N 2007 *Appl. Surf. Sci.* **253** 8725
[26] Dapor M 1996 *J. Appl. Phys.* **79** 8406
[27] Gryzinski M 1965 *Phys. Rev.* A **138** 305
[28] Gryzinski M 1965 *Phys. Rev.* A **138** 322
[29] Gryzinski M 1965 *Phys. Rev.* A **138** 336
[30] Bethe H A 1933 *Handbuch der Physik* (Berlin: Springer)
[31] Kanaya K and Okayama S 1972 *J. Phys. D: Appl. Phys.* **5** 43
[32] Penn D R 1987 *Phys. Rev.* B **135** 482
[33] Ashley J C 1990 *J. Electron Spectrosc. Relat. Phenom.* **50** 323
[34] Bouarissa N, Walker A B and Aourag H 1998 *J. Appl. Phys.* **83** 3643
[35] Chaoui Z and Bouarissa N 2002 *Phys. Lett.* A **297** 432
[36] Chaoui Z and Bouarissa N 2004 *J. Phys.: Condens. Matter* **16** 799
[37] Baker J A, Chilton N B, Jensen K O, Walker A B and Coleman P G 1991 *J. Phys.: Condens. Matter* **3** 4109
[38] Hunter K L, Snook I K and Wagenfeld H K 1996 *Phys. Rev.* B **54** 4507
[39] Coleman P G, Albrecht L, Jensen K O and Walker A B 1992 *J. Phys.: Condens. Matter* **4** 10311
[40] Aers G C 1994 *J. Appl. Phys.* **76** 1622
[41] Ghosh V J and Aers G C 1995 *Phys. Rev.* B **51** 45
[42] Sempau J, Fernandez-Varea J M, Acosta E and Salvat F 2003 *Nucl. Instrum. Methods Phys. Res.* B **207** 107
[43] Dapor M 1992 *Phys. Rev.* B **46** 618
[44] Dapor M 2008 *Surf. Interface Anal.* **40** 714
[45] Aydin A 2002 *Nucl. Instrum. Methods Phys. Res.* B **197** 11
[46] Seltzer S M 1991 *Appl. Radiat. Isot.* **42** 917
[47] Aydin A 2001 *Nukleonika* **46** 87–90
[48] Aydin A 2005 *Nukleonika* **50** 37
[49] Aydin A 2006 *Nucl. Instrum. Methods Phys. Res.* B **243** 272
[50] Zommer L, Jablonski A, Gergely G and Gurban S 2008 *Vacuum* **82** 201
[51] Dapor M 2003 *Nucl. Instrum. Methods Phys. Res.* B **202** 155